journal

J. Am. Ceram. Soc., 99 [4] 1345–1352 (2016)
DOI: 10.1111/jace.14127

Electrochemical Properties of $La_{0.5}Sr_{0.5}Co_{0.8}M_{0.2}O_{3-\delta}$ (M=Mn, Fe, Ni, Cu) Perovskite Cathodes for IT-SOFCs

Yen-Pei Fu,[‡,§,†] Adi Subardi,[‡,¶] Min-Yen Hsieh,[‡] and Wen-Ku Chang[‡]

[‡]Department of Materials Science and Engineering, National Dong Hwa University, Shou-Feng, Hualien 97401, Taiwan

[§]Nanotechnology Research Center, National Dong Hwa University, Shou-Feng, Hualien 97401, Taiwan

[¶]Department of Mechanical Engineering, STTNAS, Yogyakarta 55281, Indonesia

The electrochemical properties of $La_{0.5}Sr_{0.5}Co_{0.8}M_{0.2}O_{3-\delta}$ (M=Mn, Fe, Ni, Cu) cathodes are investigated with chemical bulk diffusion coefficients (D_{chem}) and polarization resistances. The electrochemical performance of long-term testing for $La_{0.5}Sr_{0.5}Co_{0.8}Cu_{0.2}O_{3-\delta}$ cathode was carried out to investigate its electrochemical stability. In this work, an anode-supported single cell with a thick-film SDC electrolyte (30 μm), a Ni-SDC cermet anode (1 mm), and a $La_{0.5}Sr_{0.5}Co_{0.8}Cu_{0.2}O_{3-\delta}$ cathode (10 μm) reaches a maximum peak power density of 983 mW/cm^2 at 700°C. Obviously, Cu substitution for B-site of $La_{0.5}Sr_{0.5}CoO_{3-\delta}$ cathode reduced thermal expansion coefficient (TEC) value and enhanced oxygen bulk diffusion and electrochemical properties. $La_{0.5}Sr_{0.5}Co_{0.8}Cu_{0.2}O_{3-\delta}$ is a promising cathode material for intermediate temperature solid oxide fuel cells (IT-SOFC).

I. Introduction

Recently, as electrochemical devices that directly convert the chemical energy of fuels into electricity, solid oxide fuel cells (SOFCs) have received a lot of attention due to their high electrical efficiency, fuel versatility, noise-free nature, and low-pollutant emission.[1–4] To reduce operating temperatures, it is necessary to develop new cathodes that perform well at lower temperatures (500°C–700°C). However, the conventional SOFC with the yttria-stabilized zirconia (YSZ) electrolyte and strontium-doped lanthanum manganite (LSM) cathode is not suitable for intermediate temperature solid oxide fuel cells (IT-SOFCs) due to a remarkably increase in both ohmic resistance primary from the electrolyte and polarization resistance mainly from the cathode at operating temperatures less than 700°C.[5] Mixed ionic electronic conductors (MIECs) exhibiting high ionic and electronic conductivities have been considered ideal cathodes.[6–9] Employing MIEC materials can reduce cathodic polarization resistance by extending the active zone of the reaction from the immediate three phase boundary (TPB) to part of the cathode–gas interface.[10,11] Therefore, central to IT-SOFCs is the development of alternative cathode materials with high electrocatalytic activity on oxygen reduction reactions (ORR) in order to reduce the polarization resistance at the cathodelelectrolyte interface.[12,13]

Recently, strontium-doped lanthanum–cobalt-based oxides ($La_{1-x}Sr_xCoO_3$) with high electronic conductivity and relative high oxygen ionic conductivities have received considerable attention as a promising material for IT-SOFC cathodes, and they have been identified to replace the conventional LSM material.[14–18] This is due to their high catalytic activity for the ORR, as well as their excellent electronic and ionic conductivity over a wide temperature range.[19,20] MIECs containing Mn, Fe, Ni, and Cu have demonstrated excellent catalytic performance under intermediate operating temperature conditions.[21–23] However, cobalt-containing cathodes encounter some problems such as high thermal expansion coefficients (TECs) and poor stability as well as the high cost of cobalt. Significant efforts have been devoted to optimizing catalytic activity of perovskite oxides through various ion substitutions to solve the problems of cobalt-containing cathodes and to achieve better cell performance at relatively low temperatures.[24–26] Partial substations of other elements for cobalt in cobalt-containing cathodes are considered a possible means to compensate for its disadvantages.[27] Generally, the physicochemical properties of $La_{1-x}Sr_xCoO_{3-\delta}$ (LSCO) can be altered by varying its Sr content. Based on previous research, the oxygen nonstoichiometry (δ) of LSCO increases with increasing Sr content.[28,29] Hence, the ionic conductivity and TEC of LSCO also increase.[30,31] However, the total LSCO electrical conductivity initially increases with Sr content and reaches the maximum value at $x = 0.5$. Above $x = 0.5$, the electrical conductivity decreases because of the charge compensation associated with hole consumption at higher Sr contents.[32] Therefore, LSCO with high Sr content is harmful to total electrical conductivity while simultaneously being advantageous to LSCO ionic conductivity. Consequently, a trade-off between increasing electrochemical performance and decreasing thermal expansion may be necessary to achieve optimal cathode composition.[33] In this study, $La_{0.5}Sr_{0.5}CoO_{3-\delta}$-based materials were examined, and the transition elements such as Mn, Fe, Ni, and Cu were incorporated into the B-site of $La_{0.5}Sr_{0.5}CoO_{3-\delta}$ to search the high-performance cathode for IT-SOFCs.

The electrical conductivity relaxation (ECR) technique is an easy approach to calculate the chemical bulk diffusion coefficient (D_{chem}) along with chemical surface exchange coefficient (k_{chem}) of MIECs because of the high susceptivity of the electrical conductivity changes in a variety of oxygen partial pressures.[34–39] ECR technique was used to evaluate the D_{chem} of $La_{0.5}Sr_{0.5}Co_{0.8}M_{0.2}O_{3-\delta}$ (M=Mn, Fe, Ni, Cu) cathodes. In order to study the stability of cathode polarization resistance, the long-term testing for a $La_{0.5}Sr_{0.5}Co_{0.8}Cu_{0.2}O_{3-\delta}|Ce_{0.8}Sm_{0.2}O_{1.9}$ half-cell also measured in the paper. Finally, we investigate the influence on single cell performance for transition element doping on perovskite $La_{0.5}Sr_{0.5}CoO_{3-\delta}$. The single fuel cell with a thick-film SDC electrolyte with 30 μm, a Ni-SDC cermet anode with 1 mm, and $La_{0.5}Sr_{0.5}CoO_{3-\delta}$ and $La_{0.5}Sr_{0.5}Co_{0.8}Cu_{0.2}O_{3-\delta}$ cathodes with 10 μm were fabricated to evaluate their performance.

J. Stevenson—contributing editor

Manuscript No. 37447. Received September 8, 2015; revised December 12, 2015; approved December 21, 2015.
[†]Author to whom correspondence should be addressed. e-mail: d887503@alumni.nthu.edu.tw

II. Experimental Section

(1) Preparation and Characterization of Cathode Materials

Highly pure La_2O_3, $SrCO_3$, CoO, MnO_2, Fe_2O_3, NiO, and CuO powders (>99%) were used as starting materials to prepare $La_{0.5}Sr_{0.5}CoO_{3-\delta}$ and $La_{0.5}Sr_{0.5}Co_{0.8}M_{0.2}O_{3-\delta}$ (M=Mn, Fe, Ni, Cu) cathode powders (Table I) with a solid-state reaction technique. To prepare the cathode bulk material, the $La_{0.5}Sr_{0.5}CoO_{3-\delta}$-based powders were pelletized, and then the calcined $La_{0.5}Sr_{0.5}CoO_{3-\delta}$-based cathodes were sintered in air at 1100°C for 4 h. $Ce_{0.8}Sm_{0.2}O_{1.9}$ (SDC) electrolyte powder was synthesized via coprecipitation using $Ce(NO_3)_3{\cdot}6H_2O$ and $Sm(NO_3)_3{\cdot}6H_2O$ as starting materials. This detailed procedure is outlined in another paper that our group published elsewhere.[40] The densities of the sintered samples were all greater than 95% of the theoretical density as measured by the Archimedes method.

The phase structure of the perovskites $La_{0.5}Sr_{0.5}Co_{0.8}M_{0.2}O_{3-\delta}$ (M=Mn, Fe, Ni, Cu) specimens calcined at 1000°C for 4 h were examined by a X-ray powder diffractometer (XRD; Rigaku D/MAX-2500V, Rigaku, Tokyo, Japan) by a scanning rate of 4°min^{-1} and a scanning range of 20°–80° using a CuK_α (1.5418 Å) radiation source at room temperature. The thermal expansion coefficients of the $La_{0.5}Sr_{0.5}Co_{0.8}M_{0.2}O_{3-\delta}$ (M=Mn, Fe, Ni, Cu) specimens air sintered at 1100°C were measured using a dilatometer (DIL; Model Netzsch DIL 402 PC, Bavaria, Germany) with a constant heating rate of 10°C/min in the temperature range of 25°C–600°C in air.

(2) Electrical Conductivity Test for D_{chem}

Electrical conductivity relaxation (ECR) experiments were performed on LSCO-based specimens with a typical size of 50 × 1.5 × 1.5 mm^3 and greater than 95% of the theoretical density over the temperature range of 500°C–700°C at an interval of 50°C. After stabilization at least 30 min for each temperature, a sudden change in the oxygen partial pressure, from 0.21 to 0.05 atm, was achieved by flowing O_2 and Ar into the sample chamber and altering their respective flow rates using two mass flow controllers. The electrical conductivity relaxation curve was plotted as $\frac{\sigma(t)-\sigma(0)}{\sigma(\infty)-\sigma(0)}$ vs. t. The values for D_{chem} could be determined by fitting the ECR curves.[41] The experimental details have been reported in an earlier publication.[42–44]

(3) Symmetrical Cell and Long-Term Testing

$La_{0.5}Sr_{0.5}CoO_{3-\delta}$-based cathodes were used as working electrode (WE) for electrochemical measurements in a symmetrical cell arrangement. The Ag reference electrode (RE) was located approximately 0.3–0.4 cm away from the WE. The Ag counter electrode (CE) was arranged on the other side of the sintered SDC disk. $La_{0.5}Sr_{0.5}CoO_{3-\delta}$-based cathodes were deposited onto both side of SDC electrolytes using the screen-print technique, and then sintered at 1000°C for 4 h in air. The symmetrical testing-cell experiments were performed in the temperature range of 600°C–850°C at intervals of 50°C in air (P_{O2}=0.21 atm). The applied frequency ranged from 100 kHz to 0.1 Hz with a perturbation amplitude of 10-mV AC signal. For long-term testing, EIS was measured at 700°C during 120 h in air. The exchange current density (i_0) values were calculated from AC impedance measurements. In this technique, i_0 was measured from the polarization resistance, R_p, of the Nyquist plot, and the total cathode polarization resistance (R_P) was determined from the intercepts with the real axis of the impedance loop. The following equation derived from the Bulter–Volmer equation is used to determine i_0 values:[45]

$$i_0 = \frac{RT\nu}{nFR_p}$$

Here, n is the total number of electrons passed in the reaction, ν reflects the number of times the rate-determining step occurs for one occurrence of the full reaction, F is the Faraday constant (F = 96500 C mol^{-1}), and R is the ideal gas constant (R = 8.31 J mol^{-1} K^{-1}). For the ORR, n and ν are generally assumed to be 4 and 1, respectively.[14] The detailed calculation procedure could refer to reference[42].

Table I. Composition and Abbreviation of $La_{0.5}Sr_{0.5}CoO_{3-\delta}$-Based Specimens

Composition	Abbreviation
$La_{0.5}Sr_{0.5}CoO_{3-\delta}$	LSCO
$La_{0.5}Sr_{0.5}Co_{0.8}Mn_{0.2}O_{3-\delta}$	LSCO(Mn)
$La_{0.5}Sr_{0.5}Co_{0.8}Fe_{0.2}O_{3-\delta}$	LSCO(Fe)
$La_{0.5}Sr_{0.5}Co_{0.8}Ni_{0.2}O_{3-\delta}$	LSCO(Ni)
$La_{0.5}Sr_{0.5}Co_{0.8}Cu_{0.2}O_{3-\delta}$	LSCO(Cu)

(4) The Single Cell Fabrication and Their Performance

A Ni-SDC anode-supported fuel cells were fabricated to evaluate the effect of transition elements doped on B-site of $La_{0.5}Sr_{0.5}CoO_{3-\delta}$ cathode on the performance of the single fuel cells. The Ni-SDC cermet anode was prepared by a mixture of 58 wt% NiO, 38 wt% SDC, and 5 wt% graphite. SDC powder as electrolyte was then added onto the prepressed green Ni-SDC cermet anode. Next, the SDC powders and Ni-SDC cermet anode were copressed to form a green bilayer. They were subsequently cosintered at 1400°C for 4 h to produce Ni-SDC/SDC anode-supported cell. The cathode pastes consisted of the $La_{0.5}Sr_{0.5}CoO_{3-\delta}$-based cathode powders, solvent, binder, and plasticizer were applied onto the surface of the SDC electrolyte by screen-print technique and sintered at 1000°C for 4 h. Humidified hydrogen (3 vol% H_2O) was applied as the fuel and air as the oxidant to evaluate the performance of the single cells. The current–voltage characteristics of the single cells were examined at operating temperature from 500°C to 700°C at intervals of 100°C. The single cell with a diameter of 13 mm consisted of a thick SDC electrolyte (30 μm), a Ni-SDC cermet anode (1 mm), and the $La_{0.5}Sr_{0.5}CoO_{3-\delta}$-based cathodes (10 μm).

III. Result and Discussion

(1) Structure and Thermal Expansion Behavior of Cathode Materials

The XRD patterns of $La_{0.5}Sr_{0.5}CoO_{3-\delta}$ and $La_{0.5}Sr_{0.5}Co_{0.8}M_{0.2}O_{3-\delta}$ (M=Mn, Fe, Ni, Cu) specimens calcined at 1000°C for 4 h are shown in Fig. 1. Obviously, as Cu or Fe doped on B-site of $La_{0.5}Sr_{0.5}CoO_{3-\delta}$, the perovskite structure was not significantly distorted. It can be seen that the pattern of the powders calcined at 1000°C agrees well with that of the $La_{0.5}Sr_{0.5}CoO_{2.91}$ (JCPDS card no. 48-0122). However, Ni or Mn was doped on $La_{0.5}Sr_{0.5}CoO_{3-\delta}$, some secondary phases appeared on the XRD patterns. These secondary phases may have a deleterious effect on its electrochemical properties. Thermal expansion is used to evaluate the mechanical compatibility for IT-SOFC devices among anodes, electrolytes, and cathodes at operating temperatures. A bulk thermal expansion study on $La_{0.5}Sr_{0.5}CoO_{3-\delta}$ and $La_{0.5}Sr_{0.5}Co_{0.8}M_{0.2}O_{3-\delta}$ (M=Mn, Fe, Ni, Cu) cathodes was conducted from room temperature to 600°C using a dilatometer (Fig. 2). The TEC values calculated by fitting the thermal expansion curves for LSCO, LSCO(Mn), LSCO(Fe), LSCO (Ni), and LSCO(Cu) were 21.4, 17.7, 20.6, 21.4, and 19.8 ppm/K, respectively (Table II). Clearly, doping Mn, Fe, or Cu elements into B-site of LSCO perovskite cathodes reduced the thermal expansion coefficients, whereas incorporating Ni element into

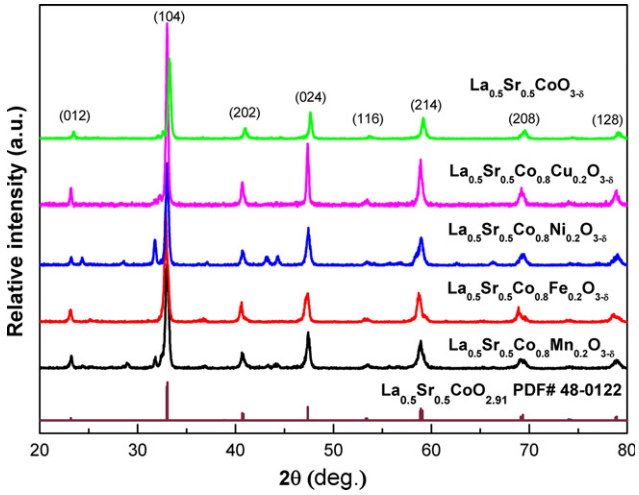

Fig. 1. X-ray diffraction patterns of $La_{0.5}Sr_{0.5}CoO_{3-\delta}$ and $La_{0.5}Sr_{0.5}Co_{0.8}M_{0.2}O_{3-\delta}$ (M=Mn, Fe, Ni, Cu) specimens calcined at 1000°C for 4 h.

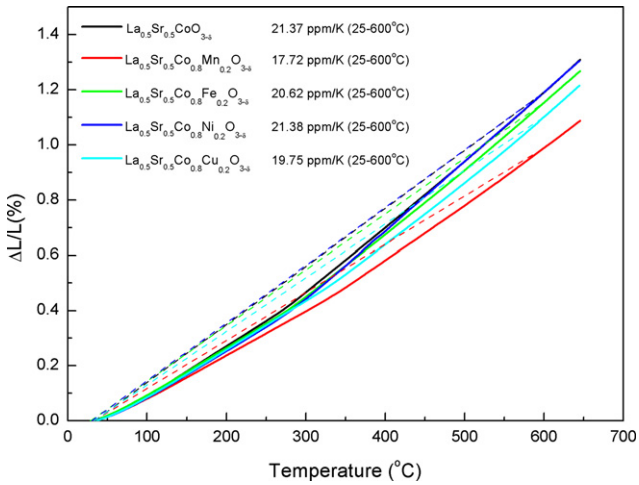

Fig. 2. Thermal expansions of $La_{0.5}Sr_{0.5}CoO_{3-\delta}$ and $La_{0.5}Sr_{0.5}Co_{0.8}M_{0.2}O_{3-\delta}$ (M=Mn, Fe, Ni, Cu) specimens as a function of temperature range of 25°C–600°C.

Table II. Thermal Expansion Coefficients of $La_{0.5}Sr_{0.5}CoO_{3-\delta}$-Based Specimens Over the Temperature Range of 25°C–650°C

Specimens	TEC (ppm/K)
LSCO	21.37
LSCO(Mn)	17.72
LSCO(Fe)	20.62
LSCO(Ni)	21.38
LSCO(Cu)	19.75

LSCO increased its thermal expansion coefficient. This is due to the fact that the larger ionic size of Ni^{2+} relative to that of Co^{3+} with high spin. Based on Shannon's report, the ionic radii of Co^{3+} with high spin and Ni^{2+} cations with coordination number of 6 are 0.61 and 0.69 Å.[46] The thermal expansion curves deviated from linearity in some degrees as shown in LSCO-based cathodes at approximately 300°C for which temperature is not associated with a phase transition. Based on our pervious report,[47] the high-temperature lattice expansion was associated with the loss of lattice oxygen. The formation of oxygen vacancies may be ascribed as follows: (1) the repulsion force arising among mutually exposed cations when oxygen ions were extracted from the lattice; and (2) the increase in cation size was due to the reduction of the Co ions from Co^{4+} to Co^{3+} or Co^{3+} to Co^{2+} valences. These must occur concurrently with the creation of oxygen vacancies to maintain electrical neutrality.[48]

(2) D_{chem} of Cathode Materials

D_{chem} was measured using the ECR technique according to variations in ambient atmosphere, leading to a change in the MIEC oxygen vacancy concentration. The suddenly change in the oxygen partial pressure of the surrounding atmosphere induces a corresponding change in the charge carrier concentration (oxygen vacancy) because of the local electroneutrality requirement.[49] Figure 3 shows normalized conductivity relaxation plots for LSCO-based cathodes for reduction step at various temperatures after an abrupt change in the oxygen partial pressure from 0.21 to 0.05 atm. The electrical conductivity relation curves were fit to equations published elsewhere.[50] Clearly it can be seen that the time to reach equilibrium increases as the temperature is reduced. Noticeably, LSCO(Cu) was revealed to be the fastest one to reach the steady state suggests that substituting Cu^{2+} for Co^{3+} resulted in a faster bulk diffusion coefficient when compared to LSCO. The main reason can be described as follows. The electron conduction is highly influenced by the overlapping between O 2*p* and the transition-metal 3*d* orbitals. The extent of the overlap strength depends on the B–O distance. In this study, the average B–O distance of Cu-O (2.00 Å) is larger than Co-O (1.93 Å). Therefore, the diffusion coefficients of LSCO-based specimens markedly correspond with the distance of B–O.[47] The D_{chem} values for LSCO, LSCO(Mn), LSCO(Fe), LSCO(Ni), and LSCO(Cu) were 1.21×10^{-5}, 0.55×10^{-5}, 0.79×10^{-5}, 0.73×10^{-5}, and 1.25×10^{-5} cm^2/s at 600°C, respectively. The detailed D_{chem} values regarding LSCO-based cathodes in the reduction process listed in Table III. The equations of D_{chem} in the temperature range of 500°C–700°C are listed as follows.

$$D_{chem} = 4.71 \times 10^{-5} \exp\left(-\frac{63.4\text{kj mol}^{-1}}{RT}\right)(m^2 s^{-1}) \text{for LSCO;}$$

$$D_{chem} = 1.62 \times 10^{-5} \exp\left(-\frac{63.6\text{kj mol}^{-1}}{RT}\right)(m^2 s^{-1}) \text{for LSCO(Mn);}$$

$$D_{chem} = 1.47 \times 10^{-5} \exp\left(-\frac{49.0\text{kj mol}^{-1}}{RT}\right)(m^2 s^{-1}) \text{for LSCO(Fe);}$$

$$D_{chem} = 1.69 \times 10^{-5} \exp\left(-\frac{53.2\text{kj mol}^{-1}}{RT}\right)(m^2 s^{-1}) \text{for LSCO(Ni);}$$

$$D_{chem} = 3.44 \times 10^{-5} \exp\left(-\frac{44.4\text{kj mol}^{-1}}{RT}\right)(m^2 s^{-1}) \text{for LSCO(Cu);}$$

The activation energy of D_{chem} calculated based on the slopes of the Arrhenius plots (D_{chem} vs. 1000/T) for LSCO, LSCO(Mn), LSCO(Fe), LSCO(Ni), and LSCO(Cu) were 63.4, 63.6, 49.0, 53.2, and 44.4 kJ/mol (Fig. 4). The activation energy is relevant to the enthalpy of defect mobility involved the equilibration between O_2 and LSCO-based cathodes.[51] This behavior results from the effect of the oxygen partial pressure, which is significantly related to defect

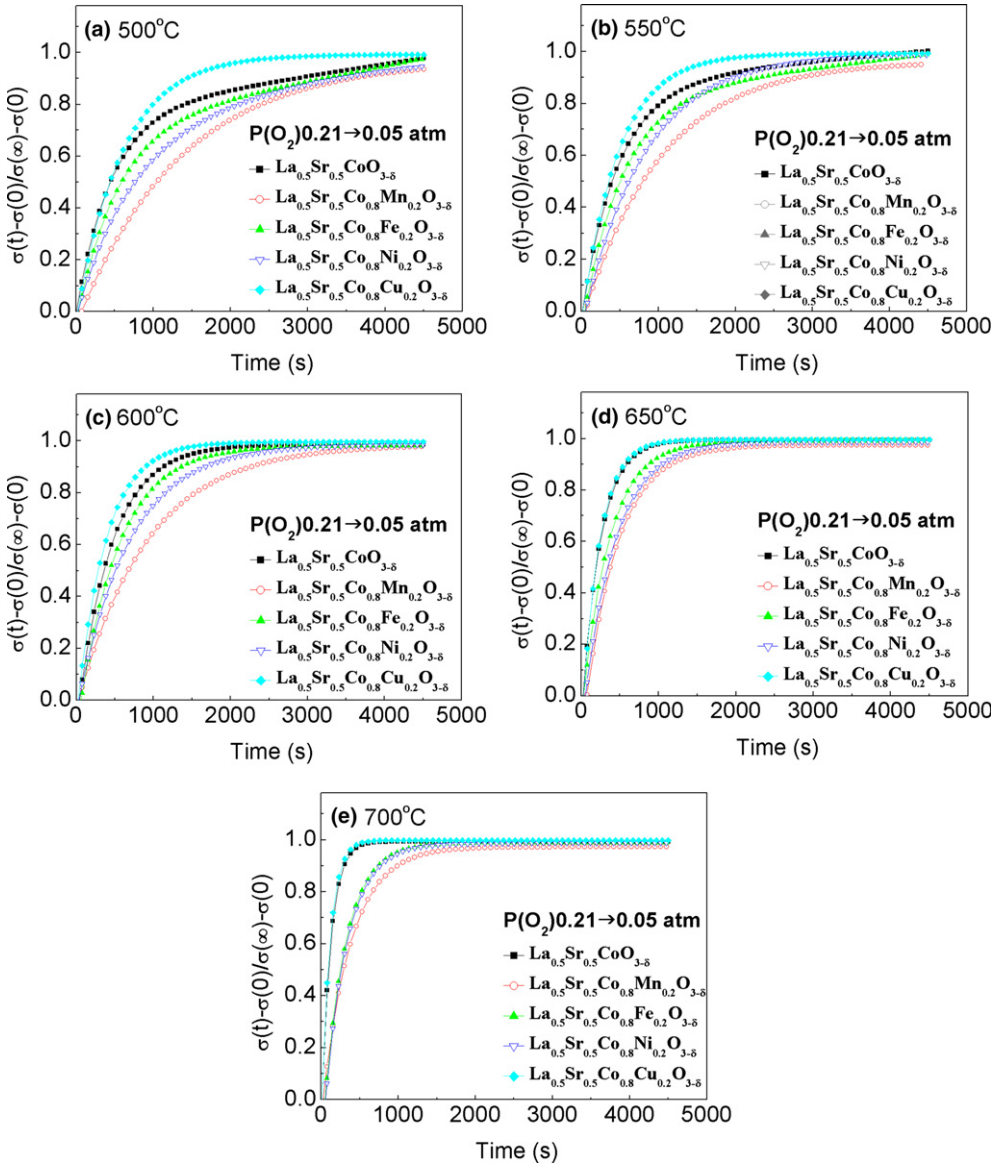

Fig. 3. The electrical conductivity relaxation curve for $La_{0.5}Sr_{0.5}CoO_{3-\delta}$ and $La_{0.5}Sr_{0.5}Co_{0.8}M_{0.2}O_{3-\delta}$ (M=Mn, Fe, Ni, Cu) specimens at (a) 500°C, (b)550°C, (c) 600°C, (d) 650°C, and (e)700°C after the oxygen pressure suddenly changed from 0.21 to 0.05 atm.

Table III. D_{chem} Values of $La_{0.5}Sr_{0.5}CoO_{3-\delta}$-Based Specimens Calculated from the Electrical Conductivity Relaxation Curve When the Oxygen Partial Pressure Abruptly Changed From 0.21 to 0.05 atm

	D_{chem} (cm^2/s)				
Specimen	500°C	550°C	600°C	650°C	700°C
LSCO	6.01×10^{-6}	8.33×10^{-6}	1.21×10^{-5}	2.33×10^{-5}	4.71×10^{-5}
LSCO(Mn)	2.37×10^{-6}	3.77×10^{-6}	5.49×10^{-6}	1.33×10^{-5}	1.62×10^{-5}
LSCO(Fe)	3.62×10^{-6}	4.72×10^{-6}	7.94×10^{-6}	1.43×10^{-5}	1.47×10^{-5}
LSCO(Ni)	3.09×10^{-6}	6.07×10^{-6}	7.28×10^{-6}	1.40×10^{-5}	1.69×10^{-5}
LSCO(Cu)	7.91×10^{-6}	9.45×10^{-6}	1.25×10^{-5}	1.86×10^{-5}	3.44×10^{-5}

concentrations, and the interactions degree between mobility and defects.[51]

(3) Performance of Symmetrical Cells and Long-Term Testing

Figure 5 presents some typical impedance spectra measured in a symmetric configuration of LSCO-based cathodes|SDC electrolyte|LSCO-based cathodes under open-circuit conditions at various temperatures in stationary air. Noticeably, when the operating temperatures were at any temperature, the LSCO(Cu) always exhibited the minimum R_p values among the LSCO-based cathodes. Table IV lists the detailed information regarding R_p values of LSCO-based cathodes at various temperatures. The R_p values of LSCO decreased from 0.92 Ω cm^2 at 600°C to 0.032 Ω cm^2 at 800°C. Similarly, the R_p values of LSCO(Cu) decreased from 0.60 Ω cm^2 at 600°C to 0.027 Ω cm^2 at 800°C. Compared with the LSCO

and the LSCO(Cu), the R_p values were slightly reduced by approximately 10% and 15% at 700°C and 800°C, respectively. After incorporating Cu in B-site of LSCO, the electrochemical processes were slightly improved such as the electrochemical reactions between the cathode and electrolyte interface, and the adsorption–desorption of oxygen diffusion between the gas and cathode surface interface. This behavior may be closely associated with low D_{chem} activation energy for LSCO(Cu).

In order to measure the long-term performance of a LSCO(Cu)|SDC half-cell, the EIS, R_p and i_0 were recorded as a function of time under stationary air as the oxidant at 700°C (Fig. 6). Obviously, R_p increased gradually with time, which values were increased from 0.094 to 0.172Ω cm^2 for

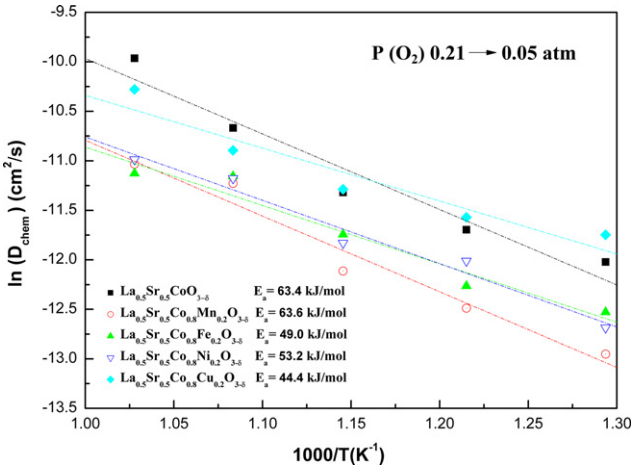

Fig. 4. Arrhenius plots of D_{chem} vs. 1000/T for the $La_{0.5}Sr_{0.5}Co_{0.8}M_{0.2}O_{3-\delta}$ (M=Mn, Fe, Ni, Cu) specimens over the temperature range of 500°C–700°C.

Table IV. Polarization Resistance of $La_{0.5}Sr_{0.5}CoO_{3-\delta}$-Based Cathodes Calculated from Nyquist Plots

	R_P (Ω cm^2)				
Specimen	600°C	650°C	700°C	750°C	800°C
LSCO	0.92	0.17	0.10	0.064	0.032
LSCO(Mn)	1.46	0.68	0.43	0.220	0.180
LSCO(Fe)	1.24	0.49	0.30	0.190	0.140
LSCO(Ni)	1.80	1.23	0.59	0.410	0.280
LSCO(Cu)	0.60	0.16	0.09	0.047	0.027

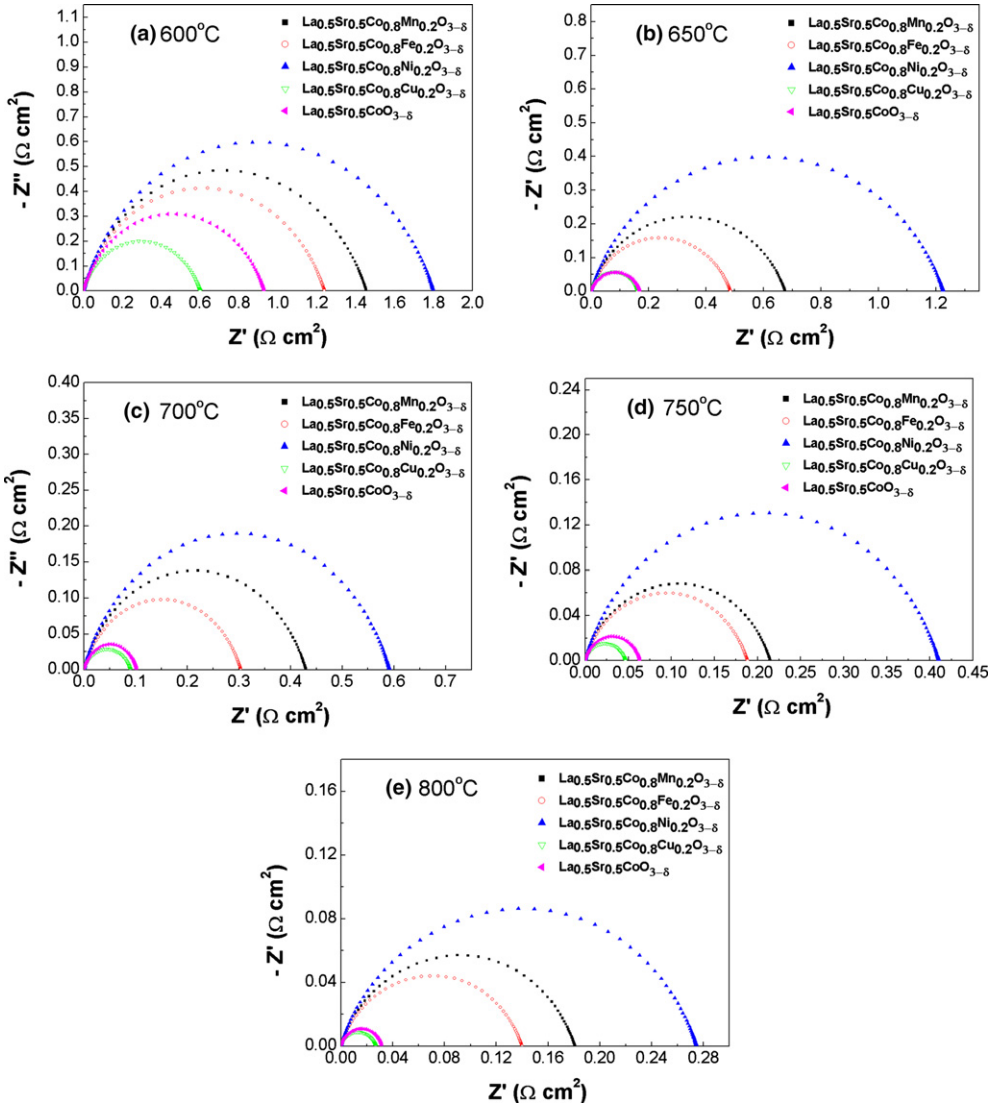

Fig. 5. Nyquist diagram of the impedance spectroscopy for $La_{0.5}Sr_{0.5}Co_{0.8}M_{0.2}O_{3-\delta}$ (M=Mn, Fe, Ni, Cu) cathodes at (a) 600°C, (b) 650°C, (c) 700°C, (d) 750°C, and (e) 800°C in air.

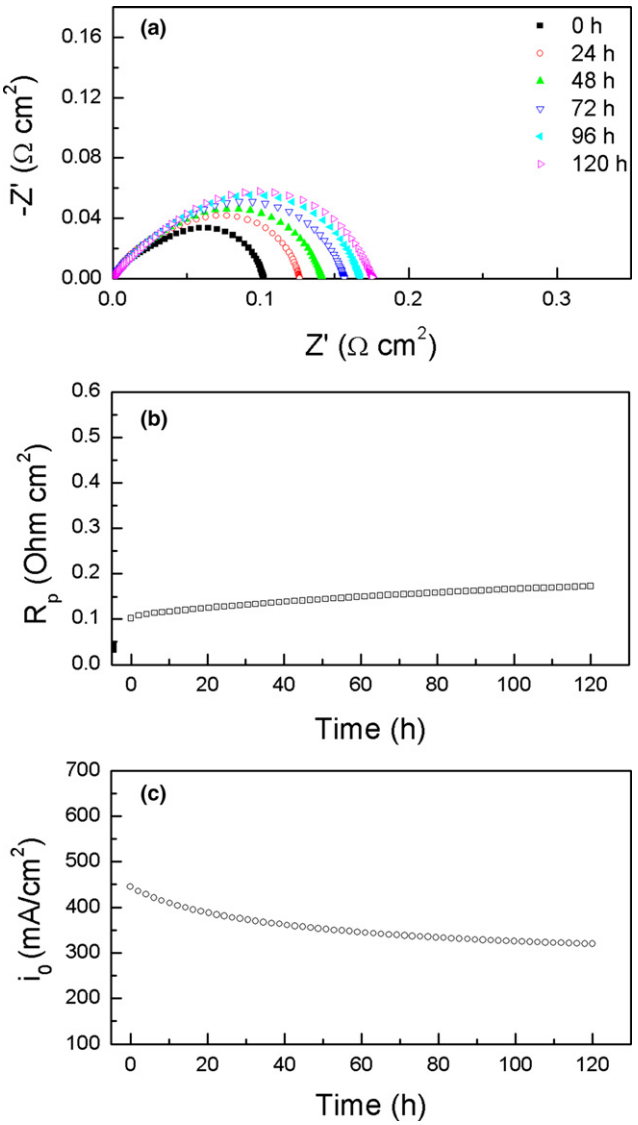

Fig. 6. Long-term testing for a $La_{0.5}Sr_{0.5}Co_{0.8}Cu_{0.2}O_{3-\delta}$|$Ce_{0.8}Sm_{0.2}O_{1.9}$ half-cell: (a) Nyquist diagram of the impedance spectroscopy, (b) polarization resistance (R_p), and (c) exchange current density (i_0).

Table V. Long-Term Testing of $La_{0.5}Sr_{0.5}Co_{0.8}Cu_{0.2}O_{3-\delta}$ Cathodes for R_p and i_0 Using the EIS Technique at 700°C

	Time					
	0 h	24 h	48 h	72 h	96 h	120 h
R_p (Ω cm^2)	0.094	0.127	0.143	0.156	0.164	0.172
i_o (mA/cm^2)	445	381	353	336	326	319

120 h long-term testing at 700°C. Similarly, i_0 decreased gradually with time, which values were decreased from 445 to 319 mA/cm^2 after 120 h long-term testing. The detailed values regarding the R_p and i_0 with various time are listed in Table V. However, these values are still acceptable to apply to the cathode for IT-SOFC. Based on our previous study,[44] the TEC value of SDC is 12.37 ppm/K, the LSCO (Cu) is 19.75 ppm/K. There is a large difference in TEC values between cathode and electrolyte. Therefore, the main reason for the half-cell performance gradually decreased may be due to cathode delamination. Moreover, Gazzarri et al. also reported the behavior is closely related to cathode delamination.[52]

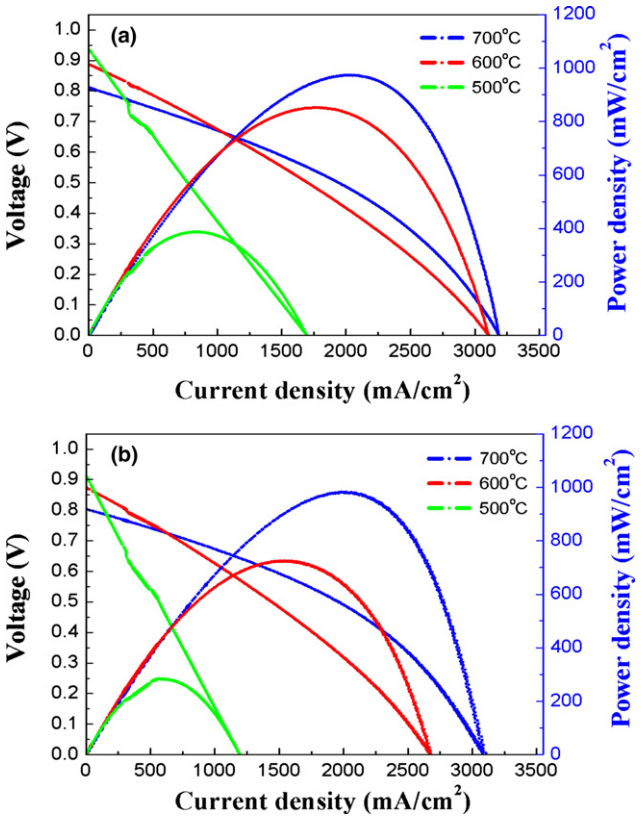

Fig. 7. The I–V curves and corresponding power densities for (a) Ni-SDC|SDC| LSCO and (b) Ni-SDC|SDC|LSCO(Cu) using hydrogen as fuel and air as oxidant in the temperature range of 500°C–700°C.

Table VI. The Peak Power Densities for Ni-SDC|SDC| LSCO and Ni-SDC|SDC|LSCO(Cu) Single Cells

	The peak power density (mW/cm^2)	
T (°C)	Ni-SDC|SDC|LSCO	Ni-SDC|SDC|LSCO(Cu)
500°C	387	284
600°C	852	725
700°C	974	983

(4) Single Cells Performance

According to the electrochemical properties of LSCO-based cathodes, LSCO and LSCO(Cu) were chosen to assemble single cells and to measure their performance. Figure 7(a) shows the single cell performance of Ni-SDC|SDC|LSCO at various operating temperatures. The peak power densities were 387, 852, and 974 mW/cm^2 at 500°C, 600°C, and 700°C, respectively. As for performance of Ni-SDC|SDC|LSCO(Cu) single cell, the peak power densities were 284, 725, and 983 mW/cm^2 at 500°C, 600°C, and 700°C, respectively [Fig. 7(b)]. Table VI summarizes the peak power densities of LSCO and LSCO(Cu) cathodes assembling anode-supported single cells over a temperature range of 500°C–700°C. Clearly, LSCO cathode assembling single cells exhibited higher peak power density at operating temperatures below 700°C compared with other literatures. For examples, Adijanto et al. reported that $La_{0.8}Sr_{0.2}CoO_{3-\delta}$ cathode exhibited max power densities about 300 mW/cm^2 at 700°C.[53] Choi et al. proposed that $La_{0.6}Sr_{0.4}CoO_{3-\delta}$ revealed max power densities of 492 mW/cm^2 at 600°C.[54] In this study, LSCO(Cu) cathode exhibits the highest peak power density of 983 mW/cm^2 at 700°C. In conclusion, LSCO(Cu) is a potential cathode for IT-SOFCs. Cu substitution for B-site of $La_{0.5}Sr_{0.5}CoO_{3-\delta}$ cathode

reduced thermal expansion coefficient (TEC) value and enhanced oxygen bulk diffusion, electrochemical properties under typical fuel cell operating conditions.

IV. Conclusions

In this study, the oxygen diffusion coefficient and electrochemical properties of $La_{0.5}Sr_{0.5}CoO_{3-\delta}$-based cathodes were investigated. The values of D_{chem} for LSCO(Cu) is 1.25×10^{-5} cm^2/s at 600°C, which is slightly greater that of LSCO at the same temperature. Doping Cu^{2+} ions on B-site of LSCO cathode exhibits higher electrochemical performances and higher single cell performances when compared to the LSCO cathode. For long-term testing, R_p of LSCO (Cu) was gradually increased from 0.094 to 0.172 Ω cm^2 after 120 h testing at 700°C, and i_0 was gradually decreased from 445 to 319 mA/cm^2 after 120 h. The peak power densities of LSCO(Cu) cathode assembling SOFC single cells were 284, 725, and 983 mW/cm^2 at 600°C, 700°C, and 800°C, respectively. A peak power density of Ni-SDC|SDC|LSCO(Cu) single cell reached 983 mW/cm^2 at 700°C. Cu substitution in the B-site of LSCO cathode reduced TEC value and enhanced oxygen bulk diffusion, electrochemical properties, and power density of anode-supported single cells. Therefore, LSCO(Cu) is considered a promise cathode for IT-SOFCs.

Acknowledgments

The authors are grateful for the financial support of this research by the Ministry of Science and Technology of Taiwan under contract number: MOST 103-2113-M-259-002 and MOST 103-2120-M-259-001.

References

[1]M. B. Choi, K. T. Lee, H. S. Yoon, S. Y. Jeon, E. D. Wachsman, and S. J. Song, "Electrochemical Properties of Ceria-Based Intermediate Temperature Solid Oxide Fuel Cell Using Microwave Heat-Treated $La_{0.1}Sr_{0.9}Co_{0.8}Fe_{0.2}O_{3-\delta}$ as a Cathode," *J. Power Sources*, **220**, 377–82 (2012).

[2]T. Hong, L. Zhang, F. Chen, and C. Xia, "Oxygen Surface Exchange Properties of $La_{0.6}Sr_{0.4}Co_{0.8}Fe_{0.2}O_{3-\delta}$ Coated With $Sm_xCe_{1-x}O_{2-\delta}$," *J. Power Sources*, **218**, 254–60 (2012).

[3]F. Meng, T. Xia, J. Wang, Z. Shi, and H. Zhao, "Praseodymium-Deficiency $Pr_{0.94}BaCo_2O_{6-\delta}$ Double Perovskite: A Promising High Performance Cathode Material for Intermediate-Temperature Solid Oxide Fuel Cells," *J. Power Sources*, **293**, 741–50 (2015).

[4]D. S. Khaerudini, et al., "Evaluation of $(Bi_{0.4}Sr_{0.6})_xCo_{0.3}Fe_{0.7}O_{3-\delta}$ (x = 0.7, 0.8, 0.9, 1.0, 1.1) Perovskite-Type Oxide as Potential Cathode for Intermediate-Temperature Solid Oxide Fuel Cells," *Int. J. Hydrogen Energy*, **40**, 11011–21 (2015).

[5]T. Horita, K. Yamaji, M. Ishikawa, N. Sakai, H. Yokokawa, and T. Kawada, "Actives Sites Imaging for Oxygen Reduction at $La_{0.9}Sr_{0.1}MnO_{3-x}$/Yttria-Stabilized Zirconia Interface by Secondary-Ion Mass Spectrometry," *J. Electrochem. Soc.*, **145**, 3196–202 (1998).

[6]P. N. Dyer, R. E. Richards, S. L. Russck, and D. M. Taylor, "Ion Transport Membrane Technology for Oxygen Separation and Syngas Production," *Solid State Ionics*, **134**, 21–33 (2000).

[7]J. P. P. Huijsmans, F. P. F. Van Berkel, and G. M. Christie, "Intermediate Temperature SOFC – A Promise for the 21st Century," *J. Power Sources*, **71**, 107–10 (1998).

[8]B. C. H. Steele, K. M. Hori, and S. Uchino, "Kinetic Parameters Influencing the Performance of IT-SOFC Composite Electrodes," *Solid State Ionics*, **135**, 445–50 (2000).

[9]W. Zhou, et al., "$Ba_{0.5}Sr_{0.5}Co_{0.8}Fe_{0.2}O_{3-\delta}$+$LaCoO_3$ Composite Cathode for $Sm_{0.2}Ce_{0.8}O_{1.9}$-Electrolyte Based Intermediate-Temperature Solid-Oxide Fuel Cell," *J. Power Sources*, **168**, 330–7 (2007).

[10]Y. Takeda, R. Kanno, M. Noda, Y. Tomida, and O. Yamamoto, "Cathodic Polarization Phenomena of Perovskite Oxide Electrodes With Stabilized Zirconia," *J. Electrochem. Soc.*, **134**, 2656–61 (1987).

[11]S. B. Adler, "Factors Governing Oxygen Reduction in Solid Oxide Fuel Cell Cathodes," *Chem. Rev.*, **104**, 4791–843 (2004).

[12]L. Zhao, et al., "High Performance of Proton-Conducting Solid Oxide Fuel Cell With a Layered $PrBaCo_2O_{5+\delta}$ Cathode," *J. Power Sources*, **194**, 835–7 (2009).

[13]A. J. Jacobson, "Materials for Solid Oxide Fuel Cells," *Chem. Mater.*, **22**, 660–74 (2010).

[14]J. Liu, A. C. Co, B. Paulson, and V. I. Briss, "Oxygen Reduction at Sol–Gel Derived $La_{0.8}Sr_{0.2}Co_{0.8}Fe_{0.2}O_3$ Cathodes," *Solid State Ionics*, **177**, 377–87 (2006).

[15]X. Song, S. Lee, Y. Chen, and K. Gerdes, "Electrochemically Influenced Cation Inter-Diffusion and Co_3O_4 Formation on $La_{0.6}Sr_{0.4}CoO_3$ Infiltrated Into SOFC Cathodes," *Solid State Ionics*, **278**, 91–7 (2015).

[16]F. Shen and K. Lu, "$La_{0.6}Sr_{0.4}Co_{0.2}Fe_{0.8}O_3$ Cathodes Incorporated With $Sm_{0.2}Ce_{0.8}O_2$ by Three Different Methods for Solid Oxide Fuel Cells," *J. Power Sources*, **296**, 318–26 (2015).

[17]Y. L. Huang, C. Pellegrinelli, K. T. Lee, A. Perel, and E. D. Wachsman, "Enhancement of $La_{0.6}Sr_{0.4}Co_{0.2}Fe_{0.8}O_{3-\delta}$ Surface Exchange Through Ion Implantation," *J. Electrochem. Soc.*, **162**, F965–70 (2015).

[18]H. N. Im, M. B. Choi, B. Singh, D. K. Lim, and S. J. Song, "Investigation of Oxygen Reduction Reaction on $La_{0.1}Sr_{0.9}Co_{0.8}Fe_{0.2}O_{3-\delta}$ Electrode by Electrochemical Impedance Spectroscopy," *J. Electrochem. Soc.*, **162**, F728–35 (2015).

[19]L. Qiu, T. Ichikawa, A. Hirano, N. Imanishi, and Y. Takeds, "$Ln_{1-x}Sr_xCo_{1-y}Fe_yO_{3-\delta}$ (Ln=Pr, Nd, Gd; x = 0.2, 0.3) for the Electrodes of Solid Oxide Fuel Cells," *Solid State Ionics*, **158**, 55–65 (2003).

[20]S. J. Skinner, "Recent Advances in Perovskite-Type Materials for Solid Oxide Fuel Cell Cathodes," *Int. J. Inorg. Mater.*, **3**, 113–21 (2001).

[21]E. Ivers-Tiffee, A. Weber, and D. Herbstritt, "Materials and Technologies for SOFC-Components," *J. Eur. Ceram. Soc.*, **21**, 1805–11 (2001).

[22]E. Perry Murray, M. J. Sever, and S. A. Barnett, "Electrochemical Performance of (La,Sr)(Co,Fe)O_3–(Ce,Gd)O_3 Composite Cathodes," *Solid State Ionics*, **149**, 27–34 (2002).

[23]S. J. Skinner and J. A. Kilner, "Oxygen Diffusion and Surface Exchange in $La_{2-x}Sr_xNiO_{4+\delta}$," *Solid State Ionics*, **135**, 709–12 (2000).

[24]Q. Ma, R. Peng, Y. Lin, J. Gao, and G. Meng, "A High-Performance Ammonia-Fueled Solid Oxide Fuel Cell," *J. Power Sources*, **161**, 95–8 (2006).

[25]T. Hibino, A. Hashimoto, M. Suzuki, and M. Sano, "A Solid Oxide Fuel Cell Using Y-Doped $BaCeO_3$ With Pd-Loaded FeO Anode and $Ba_{0.5}Pr_{0.5}CoO_3$ Cathode at Low Temperatures," *J. Electrochem. Soc.*, **149**, A1503–8 (2002).

[26]Y. Huang, J. Vohs, and R. Gorte, "Fabrication of Sr-Doped $LaFeO_3$ YSZ Composite Cathodes," *J. Electrochem. Soc.*, **151**, A646–51 (2004).

[27]H. Ding and X. Xue, "$PrBa_{0.5}Sr_{0.5}Co_2O_{5+\delta}$ Layered Perovskite Cathode for Intermediate Temperature Solid Oxide Fuel Cell," *Electrochim. Acta.*, **55**, 3812–16 (2010).

[28]S. B. Adler, "Mechanism and Kinetics of Oxygen Reduction on Porous $La_{1-x}Sr_x$ $CoO_{3-\delta}$ Electrodes," *Solid State Ionics*, **111**, 125–34 (1998).

[29]T. Bak, J. Nowotny, M. Rekas, S. Ringer, and C. Sorrell, "Defect Chemistry and Electrical Properties of $La_{1-x}Sr_xCoO_{3-\delta}$ I. Defect Equilibria," *Ionics*, **7**, 360–9 (2001).

[30]H. Ullmann, N. Trofimenko, F. Tietz, D. Stöver, and A. Ahmad-Khanlou, "Correlation Between Thermal Expansion and Oxide Ion Transport in Mixed Conducting Perovskite-Type Oxides for SOFC Cathodes," *Solid State Ionics*, **138**, 79–90 (2000).

[31]D. Baskar and S. B. Adler, "High Temperature Magnetic Properties of Sr-Doped Lanthanum Cobalt Oxide ($La_{1-x}Sr_xCoO_{3-\delta}$)," *Chem. Mater.*, **20**, 2624–8 (2008).

[32]J. Mizusaki, Y. Mima, S. Yamauchi, K. Fueki, and H. Tagawa, "Nonstoichiometry of the Perovskite-Type Oxides $La_{1-x}Sr_xCoO_{3-\delta}$," *J. Solid State Chem.*, **80**, 102–11 (1989).

[33]S. Y. Park, et al., "Structural Optimization of (La, Sr)CoO_3-Based Multilayered Composite Cathode for Solid-Oxide Fuel Cells," *J. Power Sources*, **228**, 97–103 (2013).

[34]E. Bucher, A. Egger, P. Ried, W. Sitte, and P. Holtappels, "Oxygen Nonstoichiometry and Exchange Kinetics of $Ba_{0.5}Sr_{0.5}Co_{0.8}Fe_{0.2}O_{3-\delta}$," *Solid State Ionics*, **179**, 1032–5 (2008).

[35]X. Chen, et al., "Electrical Conductivity Relaxation Studies of An Epitaxial $La_{0.5}Sr_{0.5}CoO_{3-\delta}$ Thin Film," *Solid State Ionics*, **146**, 405–13 (2002).

[36]A. Zomorrodian, H. Salamati, Z. G. Lu, X. Chen, N. J. Wu, and A. Ignatiev, "Electrical Conductivity of Epitaxial $La_{0.6}Sr_{0.4}Co_{0.2}Fe_{0.8}O_{3-\delta}$ Thin Films Grown by Pulsed Laser Deposition," *Int. J. Hydrogen Energy*, **35**, 12443–8 (2010).

[37]I. Yasuda and T. Hikita, "Precise Determination of the Chemical Diffusion Coefficient of Calcium-Doped Lanthanum Chromites by Means of Electrical Conductivity Relaxation," *J. Electrochem. Soc.*, **141**, 1268–73 (1994).

[38]I. Yasuda and M. Hishinuma, "Electrical Conductivity and Chemical Diffusion Coefficient of Sr-Doped Lanthanum Chromites," *Solid State Ionics*, **80**, 141–50 (1995).

[39]I. Yasuda and M. Hishinuma, "Electrical Conductivity and Chemical Diffusion Coefficient of Strontium-Doped Lanthanum Manganites.," *J. Solid State Chem.*, **123**, 382–90 (1996).

[40]Y. P. Fu, S. B. Wen, and C. H. Lu, "Preparation and Characterization of Samaria-Doped Ceria Electrolyte Materials for Solid Oxide Fuel Cells," *J. Am. Ceram. Soc.*, **91**, 127–31 (2008).

[41]C. Huang, D. Chen, Y. Lin, R. Ran, and Z. Shao, "Evaluation of $Ba_{0.6}Sr_{0.4}Co_{0.9}Nb_{0.1}O_{3-\delta}$ Mixed Conductor As a Cathode for Intermediate-Temperature Oxygen-Ionic Solid-Oxide Fuel Cells," *J. Power Sources*, **195**, 5176–84 (2010).

[42]Y. P. Fu, J. Ouyang, C. H. Li, and S. H. Hu, "Chemical Bulk Diffusion Coefficient of $Sm_{0.5}Sr_{0.5}CoO_{3-\delta}$ Cathode for Solid Oxide Fuel Cells," *J. Power Sources*, **240**, 168–77 (2013).

[43]A. Subardi, M. H. Cheng, and Y. P. Fu, "Chemical Bulk Diffusion and Electrochemical Properties of $SmBa_{0.6}Sr_{0.4}Co_2O_{5+\delta}$ Cathode for Intermediate Solid Oxide Fuel Cells," *Int. J. Hydrogen Energy*, **39**, 20783–90 (2014).

[44]Y. P. Fu and M. Y. Hsieh, "Chemical Bulk Diffusion Coefficient of a $La_{0.5}Sr_{0.5}CoO_{3-\delta}$ Cathode for Intermediate-Temperature Solid Oxide Fuel Cells," *J. Am. Ceram. Soc.*, **97**, 3230–7 (2014).

[45]J. Piao, K. Sun, N. Zhang, X. Chen, S. Xu, and D. Zhou, "Preparation and Characterization of $Pr_{1-x}SrxFeO_3$ Cathode Material for Intermediate Temperature Solid Oxide Fuel Cells," *J. Power Sources*, **172**, 633–40 (2007).

[46]R. D. Shannon, "Revised Effective Ionic Radii and Systematic Studies of Interatomic Distances in Halides and Chalcogenides," *Acta Crystallogr. A*, **32**, 751–67 (1976).

[47]Y. P. Fu, C. H. Li, J. Ouyang, S. H. Hu, and K. W. Tay, "Electrochemical Properties of Composite $(Sm_{0.5}Sr_{0.5})(Co_{0.8}M_{0.2})O_{3-\delta}$ (M=Cu, Mn) Cathodes for Intermediate Temperature Solid Oxide Fuel Cells," *J. Electrochem. Soc.*, **159**, F426–35 (2012).

[48]L. W. Tai, M. M. Nasrallah, H. U. Anderson, D. M. Sparlin, and S. R. Sehlin, "Structure and Electrical Properties of $La_{1-x}Sr_xCo_{1-y}Fe_yO_3$. Part 1. The System $La_{0.8}Sr_{0.2}Co_{1-y}Fe_yO_3$," *Solid State Ionics*, **76**, 259–71 (1995).

[49]J. A. Lane, S. J. Benson, D. Waller, and J. A. Kilner, "Oxygen Transport in $La_{0.6}Sr_{0.4}Co_{0.2}Fe_{0.8}O_{3-\delta}$," *Solid State Ionics*, **121**, 201–8 (1999).

[50]J. E. Elshof, M. H. R. Lankhorst, and H. J. M. Bouwmeester, "Oxygen Exchange and Diffusion Coefficients of Strontium-Doped Lanthanum Ferrites by Electrical Conductivity Relaxation," *J. Electrochem. Soc.*, **144**, 1060–7 (1997).

[51]T. Bak, J. Nowotny, and C. C. Sorrel, "Chemical Diffusion in Calcium Titanate," *J. Phys. Chem. Solids*, **65**, 1229–41 (2004).

[52]J. Gazzarri and O. Kesler, "Non-Destructive Delamination Detection in Solid Oxide Fuel Cells," *J. Power Sources*, **167**, 430–41 (2007).

[53]L. Adijanto, R. Kungas, F. Bidrawn, R. J. Gorte, and J. M. Vohs, "Stability and Performance of Infiltrated $La_{0.8}Sr_{0.2}CoxFe_{1-x}O_3$ Electrodes With and Without $Sm_{0.2}Ce_{0.8}O_{1.9}$ Interlayers," *J. Power Sources*, **196**, 5797–802 (2011).

[54]H. J. Choi, K. Bae, D. Y. Jang, J. W. Kim, and J. H. Shim, "Performance Degradation of Lanthanum Strontium Cobaltite After Surface Modification," *J. Electrochem. Soc.*, **162** [6] F622–6 (2015). □